Studying protein folding with laser tweezers

C. Cecconi

Dipartimento di Fisica, Università di Modena e Reggio Emilia - Modena, Italy

E. A. Shank

Department of Microbiology and Molecular Genetics, Harvard Medical School Boston, MA, USA

S. Marqusee

Department of Molecular & Cell Biology and the Institute for Quantitative Biology University of California, Berkeley, Berkeley CA 94720-3206, USA

C. J. Bustamante

Howard Hughes Medical Institute, University of California, Berkeley, Berkeley, CA, USA

1. – Introduction

Proteins must fold into compact and unique three-dimensional structures to carry out their specific functions. If folding goes wrong, proteins become useless and often toxic molecules for living cells. Millions of people around the world suffer from diseases caused by protein misfolding, such as Gaucher's disease, Alzheimer's disease and Parkinson's disease [1, 2]. Despite its importance, our understanding of the basic rules that govern how a protein attains its native structure is still incomplete. This lack of information is partly due to the inadequacy of conventional bulk methods to study a process that is highly heterogeneous. During folding, individual molecules are thought to follow different pathways and populate different intermediate structures on their journey to the native state [3]. Such a diversity of behaviors is often blurred in the ensemble average measured

by bulk methods. In bulk experiments, the signal is always an ensemble- and time-average of the contributions of a large, de-phased population of molecules, in which the many different folding routes and non-cumulative intermediate states are often not clearly resolved. Moreover, the unfolding potential derived from these experiments is often expressed in terms of a reaction coordinate, typically the β Tanford (β_T) value, which is not easy to interpret [4].

Recent advances in single-molecule manipulation techniques, such as atomic force microscopy (AFM) and laser tweezers [5], have made it possible to revisit protein folding with a new approach. In these experiments single molecules are directly manipulated and their behavior under tension is described in terms of a well-defined reaction coordinate, namely their molecular end-to-end distance. These methods present a number of advantages over more traditional bulk techniques, allowing us: i) to monitor in real time the fluctuations between different molecular conformations and characterize directly the thermodynamics and kinetics of these processes, ii) to measure directly the potential of mean force of a molecule as a function of its extension, ii) to probe the deformability of the folded structure, iii) to characterize the entropic elasticity of the unfolded state, and iv) to measure the magnitude of the forces that hold together the protein's tertiary structure. Moreover, because of their single-molecule nature, these experiments permit the investigation of alternative, less probable folding trajectories.

The large majority of mechanical manipulation studies on protein molecules published to date have been carried out using AFM. In these studies the mechanical unfolding of long polymeric proteins —either naturally occurring [6] or biochemically synthesized [7,8]— has been characterized in terms of a variety of parameters, such as: i) unfolding forces, ii) rates of unfolding, iii) distances from the folded structure to the transition state, iv) unfolding intermediates, and v) anisotropy of the energy landscape [9-11]. These studies have provided a wealth of new information about the mechanisms by which proteins unfold under tension and allowed us to explore phenomena previously inaccessible to experimental investigation. However, because of the stiffness of the employed AFM probes, the range of forces accessible in these experiments has been limited. A typical AFM cantilever has a spring constant of about 50 pN/nm, and thus it has a root-mean square (RMS) force noise of ~ 15 pN. Such a cantilever therefore cannot be used to monitor events that typically occur at very low forces, such refolding transitions and fluctuations between different molecular conformations [12,13]. Because of this, single-molecule mechanical manipulation experiments have so far been restricted primarily to the study of the high-unfolding behavior of proteins. These experimental limitations have recently been overcome in the work published in *Science* by Cecconi *et al.* [14]. In this work, the authors present a method to manipulate individual globular proteins in the low-force regime of the laser tweezers, where optically trapped beads have a RMS force noise of less than 1 pN [14, 15]. Using this experimental approach, Cecconi and co-authors directly monitored the unfolding and *refolding* trajectories of *E. coli* ribonuclease HI (RNase H) molecules and uncovered information inaccessible to more traditional bulk techniques.

This paper provides a brief overview of the basic principles of the laser tweezers, details the experimental procedure that we devised to make globular proteins amenable

to mechanical manipulation, and describes and discusses the major results and findings of Cecconi *et al.* regarding the folding mechanism of RNase H obtained through single-molecule manipulation studies.

2. – Laser tweezers

Laser tweezers were invented by Arthur Ashkin and colleagues in 1986 when they discovered that by focusing a laser beam through a microscope objective they could trap and manipulate small particles of high refractive index, such as plastic beads and oil droplets [16]. Since its invention, laser tweezers have become a versatile tool to trap and manipulate a diverse range of small objects, from living cells down to single atoms, with many applications in biophysics and other disciplines [17, 18]. The mechanism of optical trapping for objects that are much larger than the wavelength of light can be explained through a simple ray optics model. Light photons carry momentum equal to h/λ, where h is Planck's constant and λ is the wavelength of light. When a stream of photons interacts with an object and it is either absorbed or scattered the momentum carried by light changes. Since momentum is conserved, the rate of change in momentum of the light must be equal and opposite to the rate of change in momentum of the scattering object. Because of this, a particle that acts as a positive lens and refracts light towards its center can be entrained in a light beam.

Consider a collimated beam of light with a Gaussian intensity profile hitting a refractive sphere that is situated off-axis in the beam, as shown in fig. 1a). For each ray in the beam the components of momentum flux parallel and perpendicular to the optical axis are

$$(\mathrm{d}p/\mathrm{d}t)_{\mathrm{parallel}} = n_B(W/c)\cos\theta \tag{1}$$

and

$$(\mathrm{d}p/\mathrm{d}t)_{\mathrm{transverse}} = n_B(W/c)\sin\theta, \tag{2}$$

respectively, where W is the power of the light ray, θ is the angle of the ray to the optic axis, c is the speed of light, and n_B is the refractive index of the liquid surrounding the sphere [19]. The reaction impulse (F) felt by the bead is equal but opposite to the change in the light momentum flux summed over all rays passing through the bead:

$$F_{\mathrm{bead}} = -\sum_{\mathrm{rays}} (\mathrm{d}p/\mathrm{d}t)_{\mathrm{in}} - (\mathrm{d}p/\mathrm{d}t)_{\mathrm{out}}\,. \tag{3}$$

If the bead hit by the beam of light acts as a converging lens, as shown in fig. 1a), then the strong central rays are refracted away from the beam axis, while the weaker peripheral rays are refracted towards it. This results in a net downward change of light momentum flux that causes the bead to feel a force that draws it towards the center of the beam. However, since the parallel component of the ray momentum is reduced

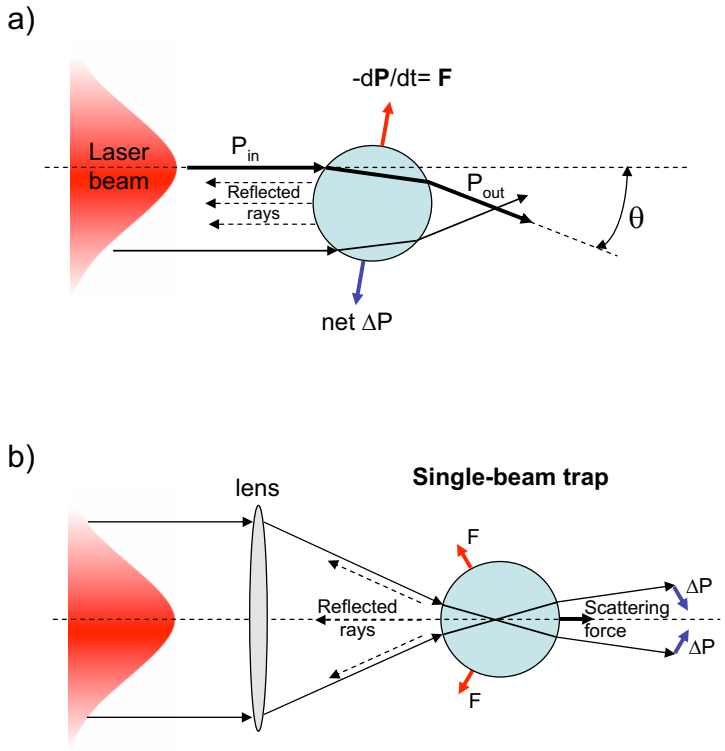

Fig. 1. – Light momentum effects on a refractive sphere. a) A collimated laser beam with a Gaussian intensity profile entrains a bead, but it also pushes it away from the light source. b) A focused laser beam with a Gaussian intensity profile traps a bead at a particular point in space. The scattering force caused by reflected rays is balanced by the refraction of the high angle rays and the particle is trapped slightly off center.

after refraction, the bead feels an additional scattering force that pushes it downstream. Additionally, the bead is scattered forward by reflected rays. Thus, when a particle is hit by a collimated beam of light with an intensity profile peaked in its center, the particle light source [20].

To trap a bead at a particular point in space, the beam of light must be focused (fig. 1b)). In this situation, a bead at the focus is pushed forward by the reflected rays until the scattering force is compensated by a backward force caused by the increase in the forward momentum flux of the rays refracted by the bead. The bead is thus trapped slightly downstream of the light focus. The larger the focal cone angle of the beam is, the stronger the backward force that opposes the axial escape of the bead is. Thus, to efficiently trap a bead with a single-beam trap, the back aperture of a high numerical aperture objective must be completely filled by the trapping beam.

In order to trap the bead at the light focus and avoid the use of large focal cone angles, dual counter-propagating laser beams with a common focal point must be used, as shown

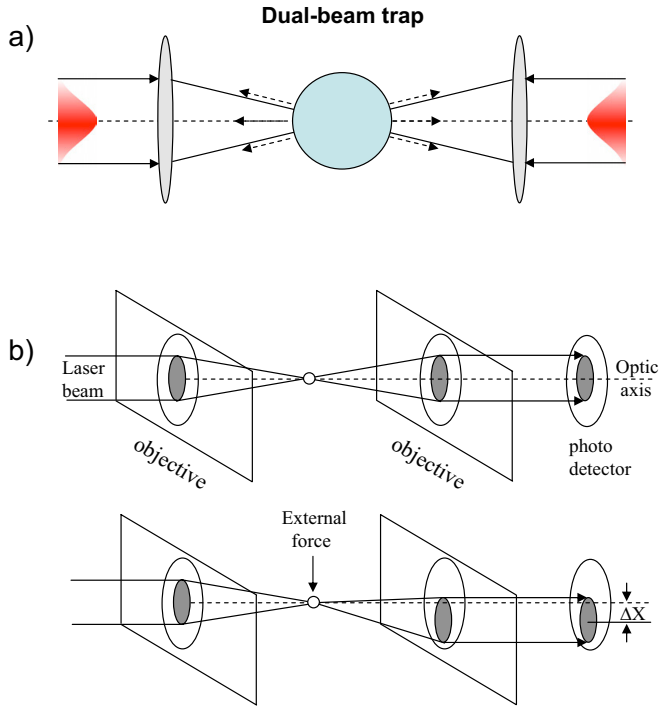

Fig. 2. – Dual counter-propagating laser beams. a) In a dual-beam trap, the scattering forces caused by reflected rays are canceled, while the gradient forces are doubled; the bead is trapped at the light focus. b) Light-momentum force sensor, based on fig. 1 of Smith *et al.* [15]. Two low numerical aperture (NA) beams are used with two high-NA objectives. Each objective is used twice: to focus one beam and collect the other beam for analysis. The narrow cones of light used in this set-up allow the collection of nearly all the light leaving the trap, even after significant deflection of the beam. When an external force is applied on the bead, the bead moves slightly downward and the light is refracted asymmetrically. By collecting all the light momentum leaving the trap it is possible to measure the force acting on the bead as $F = (W/c)(x/R_L)$, where W is the light intensity, c is the speed of light, x is the offset measured by the photodetector and R_L is the focal length of the lens [15].

in fig. 2a). In this experimental set-up, the scattering forces generated by reflected rays are canceled, while the transverse gradient forces are doubled. Using narrow cones of light with this laser tweezer configuration allowed Smith *et al.* to devise a new method for measuring optical trap forces that relies on the direct measurement of the transverse change in momentum flux of the trapping beam [15] (fig. 2b)). When a force F is applied on the trapped particle, the particle moves downward until the light pressure from the deflected beam exactly balances the external force. If narrow cones of light are used and the back aperture of the laser trap objectives is underfilled, then all the light momentum leaving the trap can be collected and directed to position-sensitive photodetectors. The offset distance measured by the photodetectors can then be transformed into the angular

deflection of light to calculate the change in the momentum flux of the trapping beam that, according to momentum conservation, equals the force applied on the particle. This force-measurement method presents several advantages over more traditional ones, being independent of the particle's size or shape, the distance beyond the cover glass, and the viscosity and refractive index of the buffer [15]. The experimental design depicted in fig. 2b) cannot be used to measure forces in a single-beam trap because a single beam of light with such small cone angle does not trap a bead efficiently.

The data shown in this paper were collected with a momentum-flux force sensor dual beam laser trap built by Steve B. Smith and detailed in Smith *et al.* [15].

3. – Synthesis of molecular constructs for use in mechanical manipulation studies

A major issue in single-molecule manipulation studies is to find conditions that facilitate the attachment of the molecule under study to movable substrates, while keeping the strength of the interactions between the tethering surfaces to a minimum. This is a difficult task to fulfill when trying to manipulate nanometer-sized globular proteins with micrometer-sized beads, such those used in laser tweezer experiments. A direct attachment of the protein molecule to the beads would require the large tethering surfaces to come so close to each other they would interact, thus compromising the measurements. To overcome this problem, we developed a new experimental procedure to make globular proteins amenable to mechanical manipulation in laser tweezer experiments [21]. This approach relies on the use of molecular handles, ~ 500 bp DNA molecules, to specifically connect the protein to polystyrene beads and keep the attachment points at a distance at which unspecific interactions between the tethering surfaces are negligible (fig. 3). One end of each DNA molecule is covalently attached to a cysteine residue of the protein through a disulfide bond, while the other end is bound to a bead through either streptavidin-biotin or digoxigenin-antibodies interactions. The thiol-thiol chemistry between the handles and the protein is mediated by 2,2′-dithiodipyridine (DTDP) [22-24]. An excess of DTDP is first used to activate cysteine-bearing proteins, which are then reacted with a mixture of the two handles to produce the DNA-protein chimeras used in laser tweezer experiments. Only 50% of the chimeras synthesized through this method have the required configuration of one biotin- and one digoxigenin-labeled handles; the rest of the molecules carry identical handles and therefore do not function in laser tweezer experiments. The time course of the disulfide bond formation can be followed spectrophotometrically at 343 nm via the release of the leaving group pyridine-2-thione. The activation of cysteine residues with DTDP is typically complete within a few minutes, whereas the attachment of the DNA molecules to the activated proteins follows slower kinetics and can take hours, or even days, to reach completion (data not shown) [21]. The success and extent of the protein/DNA coupling reaction can be assessed both by gel electrophoresis and AFM. Indeed, DNA-protein complexes run as distinct retarded bands in polyacrylamide gels, and can be easily visualized by AFM imaging, (data not shown) [21].

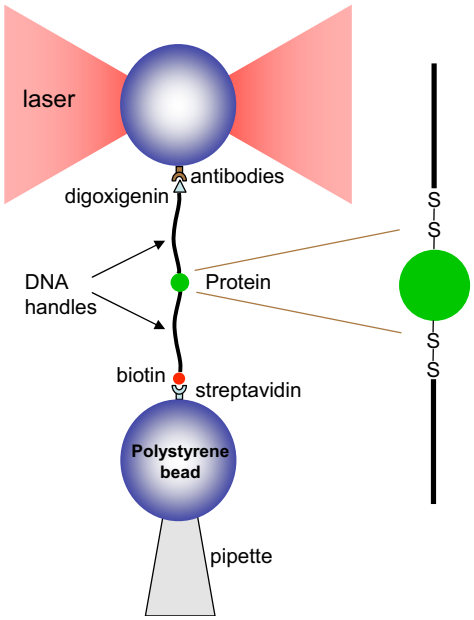

Fig. 3. – Schematic representation of the experimental set-up used to mechanically manipulate individual globular proteins by laser tweezers (not to scale). During the experiment the molecule is stretched and relaxed several times by moving the pipette relative to the optical trap and the force applied on the molecule is determined by measuring the change in momentum flux of the light beams leaving the trap. The extension of the molecule is determined using a light "lever system" [31].

To ensure that meaningful information could be obtained from the manipulation of our molecular constructs, we assessed the effect of the handles on the structure and enzymatic activity of the protein through bulk experiments. We showed that DNA-modified RNase H retains its overall fold and its enzymatic activity (fig. 4a) and b), respectively) an indication that in our laser tweezer samples the protein preserves its three-dimensional conformation [14]. This experimental procedure devised to manipulate individual RNase H molecules should be general and adaptable to the study of most proteins.

4. – Mechanical manipulation of single RNase H molecules by laser tweezers

E. coli ribonuclease HI (RNase H) is an enzyme that hydrolytically cleaves the ribonucleotide backbone of RNA-DNA hybrids in a divalent cation (Mg^{2+} or Mn^{2+}) dependent manner [25]. It is a small single-domain protein of 155 amino acids, consisting of both α-helices and β-sheets, and lacking disulfide bonds and prosthetic groups [26]. The structure, stability and folding of RNase H have been intensively studied with bulk techniques by several groups [26-28]. Despite this effort, however, crucial aspects of the folding mechanism of this protein have proven difficult to investigate with traditional en-

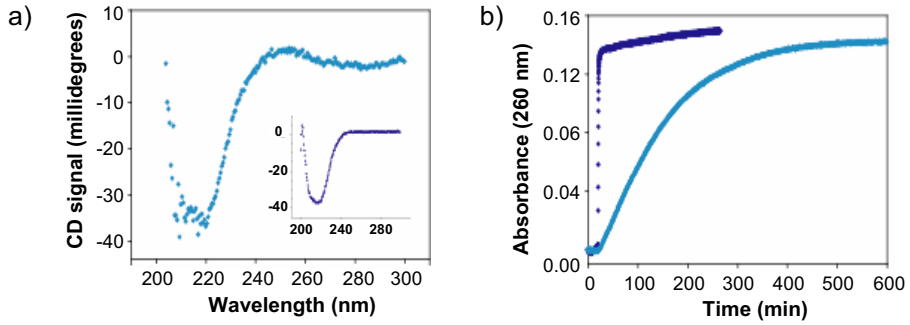

Fig. 4. – Effect of DNA handles on protein's structure and enzymatic activity. a) Circular dichroism spectra of RNase H alone (inset) and with 40 bp dsDNA molecules attached (light blue dots), adapted from Cecconi *et al.* [14]. The two spectra are very similar, indicating that the DNA-modified protein retains its overall fold. These experiments were carried out with 40 bp dsDNA because it was technically difficult to obtain enough sample with long handles (558 bp) for circular dichroism studies. b) Spectrophotometric activity assay of the protein alone (dark blue dots), and with 558 bp ds DNA attached (light blue dots). The DNA-modified protein retains its enzymatic activity; adapted from Cecconi *et al.* [14].

semble methods. For example, in bulk studies, RNase H has been observed to populate a moderately stable, partially structured kinetic intermediate, postulated to be a molten globule [29] (fig. 5). However, because this partially folded conformation forms within the dead time of the measuring instrument (12 ms), it has been difficult to establish directly

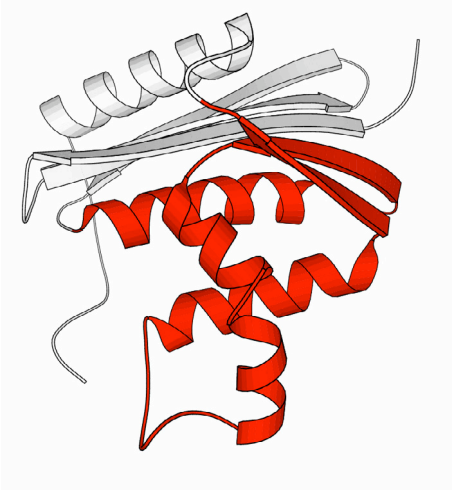

Fig. 5. – Ribbon structure of RNase H. The red region is the part of the molecule that is structured in the burst-phase intermediate as determined by pulse labeling hydrogen-deuterium exchange experiments [29].

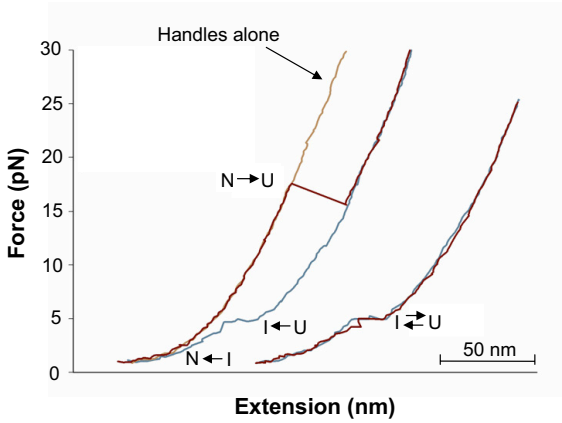

Fig. 6. – Mechanical manipulation of individual RNase H molecules. Two successive force-extension cycles obtained by pulling and relaxing the same RNase H molecule are shown; one cycle is displaced laterally for clarity, adapted from Cecconi *et al.* [14]. The stretching (red) and relaxation (blue) traces display sudden changes in extension corresponding to unfolding and refolding events of the protein. The size of the high-force stretching transition at $\sim 19\,\mathrm{pN}$ is consistent with the complete unfolding of the native state. The size of the low-force stretching and relaxation transitions at $\sim 5.5\,\mathrm{pN}$ is instead consistent with the unfolding and refolding of an intermediate, partially folded, structure. In fact, the refolding of the protein into this intermediate state does not restore the original length of the molecule, leaving a gap between the stretching and the relaxation traces at $\sim 5.5\,\mathrm{pN}$ (left curve). If the intermediate state is not given enough time at low forces to fold into the native structure, it unfolds again in next pulling cycle at about the same force at which it folded, indicating that the unfolding of I is reversible (right curve). When handles alone with no protein were pulled no transitions were observed (yellow trace).

whether this intermediate is on- or off-pathway and whether it is an obligatory step in the folding trajectory to the native state. Moreover, it has not been clear whether this intermediate is a distinct thermodynamic state or simply a redistribution of the unfolded ensemble under folding conditions [30].

With the intent of shedding light on some of these unresolved issues, we decided to reinvestigate the folding of RNase H with a new approach: using laser tweezers. Individual RNase H molecules were tethered to polystyrene beads by means of molecular handles, as depicted in fig. 3 and described above. One bead was held in a force-measuring optical trap, while the other was held by suction at the end of a micropipette connected to a piezo-electric actuator. During the experiment, the molecule was stretched and relaxed multiple times by moving the micropipette relative to the optical trap to generate force-extension curves like the one shown in fig. 6. When mechanically manipulated, RNase H unfolds in a two-state manner (native state $N \rightarrow U$ unfolded state) at $\sim 19\,\mathrm{pN}$, and refolds through an intermediate structure (I) at $\sim 5.5\,\mathrm{pN}$, which then folds into the native state at lower forces ($\sim 1\,\mathrm{pN}$). If the $I \rightarrow N$ transition fails, the intermediate is stretched in the next pulling cycle and observed to unfold at $\sim 5.5\,\mathrm{pN}$ (fig. 6, right

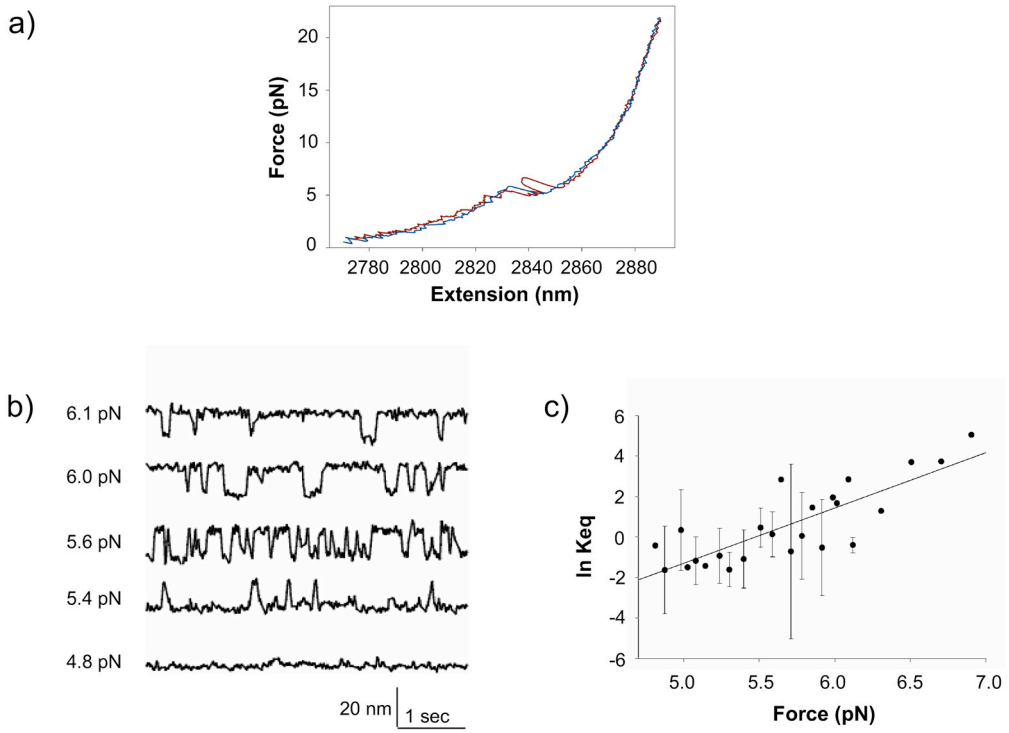

Fig. 7. – Fluctuations between the intermediate and the unfolded states. a) Force extension-curve showing interconversion between the U and I states, adapted from Cecconi *et al.* [14]. b) Extension *vs.* time traces of RNase H at various constant forces, adapted from Cecconi *et al.* [14]. When held at a force near 5.5 pN, RNase H shows bistability and hops between the intermediate and the denaturated form of the protein. By changing the preset force the $U \leftrightarrows I$ equilibrium can be shifted. c) Equilibrium constant (K_{eq}) of the $U \leftrightarrows I$ transition at any given force calculated as the ratio of the lifetimes of the U and I states, adapted from Cecconi *et al.* [14].

panel). The fact that the unfolding and refolding traces of I nearly coincide, indicates that the $U \leftrightarrows I$ transition occurs reversibly under our experimental conditions. In fact, consistent with this observation, when the molecule was manipulated slowly enough (at a speed less than 300 nm/s), the protein was sometimes observed to fluctuate between the unfolded and intermediate states during force-extension cycles (fig. 7a)). In order to investigate these fluctuations in more detail, we fixed the applied force on the molecule to a predetermined value near 5.5 pN using the force-feedback mode of the instrument, and monitored the fluctuations in extension of the molecule as a function of time. Under these experimental conditions, the molecule shows bistability, hopping between the U and I states in a force-dependent manner (fig. 7b)). From the force-dependent rates of unfolding and refolding of the intermediate —calculated as the inverse of the average life times of the I and U states— we estimated the position of the transition state between

U and I by fitting these rates with the Arrhenius-like equation:

$$k_{I\to U} = k_m {k^0}_{I\to U} \exp[F\Delta {x^\ddagger}_{I\to U}/k_{\mathrm{B}}T], \tag{4}$$

where k_m represents the contribution of the instrument to the absolute rates, ${k^0}_{I\to U}$ is the unfolding rate at zero force, F is the force applied on the molecule, $k_{\mathrm{B}}T$ is the thermal energy, and $\Delta {x^\ddagger}_{I\to U}$ is the distance from I to the transition state along the reaction coordinate [14, 31]. A similar expression holds true for the reverse $U \to I$ transition. From the slope of $\ln k$ *vs.* F plots we estimated $\Delta {x^\ddagger}_{I\to U}$ to be 5 ± 1 nm, and $\Delta {x^\ddagger}_{U\to I}$ to be 6 ± 1 nm. The distance from I to the transition state is much larger than that found for the mechanical unfolding of any protein native state studied so far ($\Delta {x^\ddagger}_{N\to U}$ is typically less than 1 nm), and it is similar to that found for the unfolding of biomolecules whose structure is mostly stabilized by secondary interactions [31]. The large $\Delta {x^\ddagger}_{I\to U}$ value, and thus the large mechanical compliance and "stretchiness" of I, could therefore reflect the intermediate state's lack of those stereospecific tertiary contacts that stabilize native structures and make them brittle under force.

From the lifetimes of the unfolded and intermediate state in constant force-experiments we could also calculate the equilibrium constant of the $U \leftrightarrows I$ transition at difference forces and then extrapolate to zero force to estimate K_{eq} ($F = 0$) (fig. 7c)). This analysis yielded a K_{eq} ($F = 0$) that corresponds to a $\Delta G_{(UI)}$ of 9 ± 1.5 kcal/mol. The change in free energy associated with the mechanical denaturation of a molecule comprises the free-energy difference between the folded and unfolded states at zero force (ΔG^0) and the free-energy change to stretch the unfolded state (ΔG_{str}) (fig. 8). Assuming the response of a polypeptide chain to force to be well described by the worm-like chain model (WLC) [32], ΔG_{str} can be calculated as the area under the WLC force-extension curve integrated from zero to the extension of the unfolded polypeptide chain; for our system ΔG_{str} was calculated to be 5 ± 1 kcal/mol [14]. After correction for ΔG_{str}, the free-energy change of the $U \leftrightarrows I$ transition measured in our experiments corresponds well with that measured in bulk studies ($\Delta G_{(UI)(\mathrm{bulk})} = 3.6 \pm 0.1$ kcal/mol).

Two other independent methods were used to evaluate the thermodynamics of the $U \leftrightarrows I$ transition. In one approach, we determined the potential of mean force of the reversible unfolding of the intermediate as the average area under the unfolding/refolding plateau; this analysis yielded $\Delta G_{(UI)} = 9 \pm 2$ kcal/mol. In the second method, we analyzed the probability of U refolding to I as a function of force using the statistics of a two-state system and obtained a $\Delta G_{(UI)}$ of 8.9 ± 0.25 kcal/mol [14]. These free-energy values, after correction for ΔG_{str}, also correlate well with $\Delta G_{(UI)(\mathrm{bulk})}$ (table I). The remarkable similarity between the free-energy value measured in ensemble experiments and those acquired at the single molecule level suggest that there is a resemblance between the intermediate structures observed using these two techniques. To further examine this similarity, we mechanically manipulated a variant of RNase H (I53D RNase H). I53D RNase H carries a point mutation in the core region of the protein that destabilizes the bulk kinetic intermediate, making the protein fold in a two-state manner [33]. In agreement with what is observed in solution, in our single molecule experiments the I53D

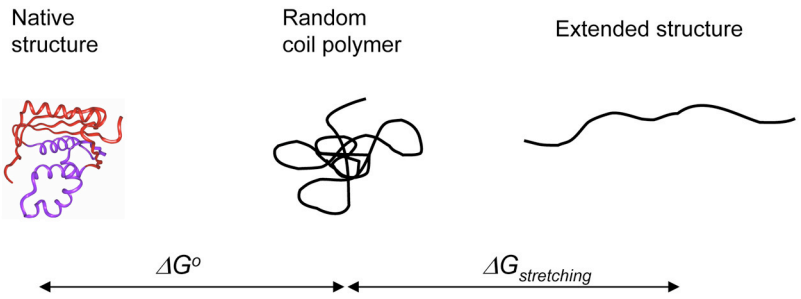

Worm-like chain interpolation formula

$$F = \frac{\kappa_B T}{p}\left[\frac{1}{4}\left(1-\frac{x}{L_c}\right)^{-2} - \frac{1}{4} + \frac{x}{L_c}\right]$$

Fig. 8. – Correcting for the stretching of the unfolded state. The Gibbs free-energy difference (ΔG) is a thermodynamic function and it thus depends only on the initial and final state of a process. The chemical and mechanical denaturation of a protein are processes that share the same initial state, namely the native structure of the molecule, but have quite different final states. In chemical denaturation experiments the final state is a random coil polymer, whereas in mechanical manipulation studies the final state is a stretched molecule. To compare free energies measured in solution with those obtained in our experiments, the work done to extend the polypeptide chain, $W = \Delta G_{\mathrm{str}}$, must be taken into account. This work can be calculated using the worm-like chain (WLC) interpolation formula: $F = (k_{\mathrm{B}}T/P)(1/(4(1-x/L)^2)+x/L-1/4)$, where P, x and L are the persistence length, end-to-end distance and contour length of the molecule, respectively [32]. This formula has been shown to describe well the behavior of a polypeptide chain under tension [34].

variant refolds through a gradual compaction rather than a sharp transition, showing no evidence of an intermediate state (fig. 9). This data further support the idea of identity between the mechanical and bulk intermediates and make our findings relevant to the folding process of RNase H in solution. We could therefore use laser tweezers to answer questions that more traditional techniques had failed to address. The interconversion between the intermediate and the unfolded states during constant force measurements appears to be a first-order process, as indicated by the distributions of the dwell times of the I and U states (fig. 10). These results, together with the sharpness of the $U \leftrightarrows I$ transitions and the narrowness of the unfolding and refolding force distributions of I (data not shown) suggest that the intermediate that populates the refolding trajectories of RNase H is a well-defined, compact, thermodynamically distinct molecular structure, probably held together mostly by local interactions.

TABLE I. – *Comparison between the change in free energies for the* $U \rightleftharpoons I$ *transition measured in bulk and in single-molecule mechanical studies.*

	Bulk experiments	Laser tweezer experiments
$\Delta G_{(UI)}$	3.6 ± 0.1 kcal/mol	3.8 ± 0.82 kcal/mol 4 ± 2.6 kcal/mol 4 ± 2 kcal/mol

The interconversion between the intermediate state and the unfolded state was sometimes observed to stop during constant force measurements (fig. 11). This arrest was always associated with a downward step in the extension *vs.* time trace corresponding to a decrease in the end-to-end distance of the molecule. This molecular compaction well corresponded to that expected for the I to N transition at the given forces. In fact, when the molecule was stretched after hopping had ceased, we always observed a high force event at ~ 19 pN, corresponding to the $N \rightarrow U$ transition, and not the unfolding of the intermediate state at ~ 5.5 pN. Thus, during constant force experiments, we were sometimes able to directly observe the molecule cross the folding barrier to the native state. In about 80% of these cases, the jump into the native structure clearly took place from the intermediate state, as in fig. 11. In the rest of the cases, I might have been too short-lived to be resolved in our measurements. These data indicate that the refolding intermediate observed in our experiments is on-pathway. Moreover, since all our force-extension curves display the low-force $U \rightarrow I$ transition, the same intermediate also appears to be an obligatory step in the refolding trajectories of RNase H.

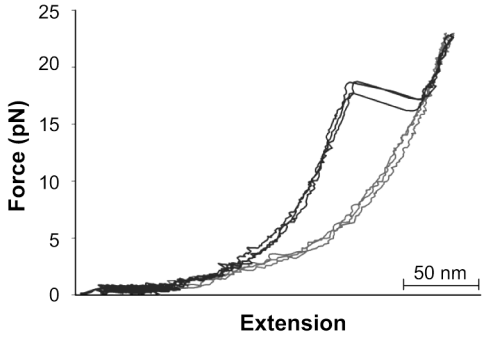

Fig. 9. – Force-extension curves for the I53D RNase H variant, from Cecconi *et al.* [14]. This mutant refolds gradually, showing no low force refolding or unfolding transitions (compare behavior at ~ 5.5 pN to that shown in fig. 6).

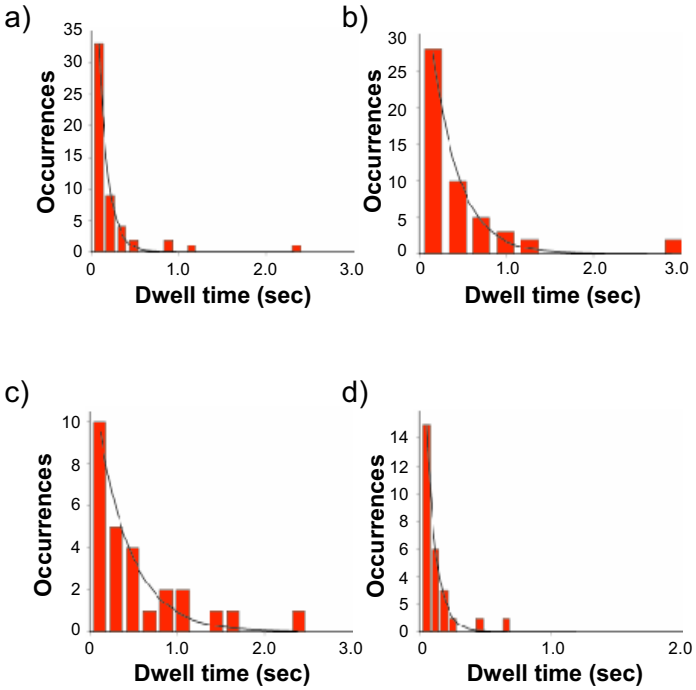

Fig. 10. – Dwell time distributions of the unfolded and intermediate states of RNase H during constant force measurements, adapted from Cecconi *et al.* [14]. The distributions are well fit by single exponentials, revealing the first-order nature of the $U \leftrightarrows I$ transition. From these fits we estimated the unfolding and refolding rate constants of the intermediate. At force equal to 5.1 pN, the $U \rightleftharpoons I$ equilibrium is shifted toward I with $k_f = 9.1 \pm 0.5\,\mathrm{s}^{-1}$ and $k_u = 3.27 \pm 0.24\,\mathrm{s}^{-1}$, panel a) and b), respectively. Instead, at 5.9 pN the unfolded state predominates and $k_f = 2.6 \pm 0.35\,\mathrm{s}^{-1}$ and $k_u = 13.1 \pm 0.68\,\mathrm{s}^{-1}$, panel c) and d), respectively.

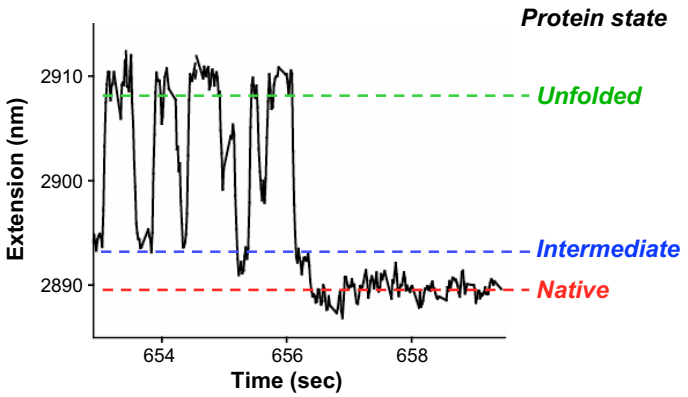

Fig. 11. – Extension *vs.* time traces of RNase H, adapted from Cecconi *et al.* [14]. The molecule is directly observed to fold into the native structure from the intermediate state.

5. – Conclusion

Protein folding is thought to be a very heterogeneous process where individual molecules fold into their native state through many different pathways on a multidimensional funnel-shaped energy landscape [3]. The experimental characterization of such a multitude of folding routes requires measurements at the single-molecule level, since ensemble measurements provide only average information about the folding process. In this paper we describe an experimental approach to study protein folding at single-molecule level. This method relies on the use of molecular handles to mechanically manipulate individual globular proteins in the low force regime of optical tweezers. In these experiments, single molecules are stretched and relaxed multiple times and their behavior under tension is described as a function of their molecular end-to-end distance. The low spring constant of the laser trap allows the manipulation of the molecules at close to equilibrium conditions and the direct monitoring of fluctuations between different molecular conformations. We applied this experimental approach to study the folding mechanism of RNase H. We characterized the complete mechanical unfolding and refolding trajectories of individual RNase H molecules and identified a refolding intermediate (I) that correlates with the conformation sampled in ensemble studies, which has been postulated to be a molten globule. Unlike in bulk experiments where I forms within the dead time of the measuring instruments, in our measurements the interconversion between the intermediate and the unfolded states could be monitored and visualized in real time, allowing us to characterize directly the kinetic, thermodynamic and mechanical properties of this molten globule. We demonstrated that the intermediate that populates the folding trajectories of RNase H is a compact, thermodynamically distinct state, which is both obligatory and on-pathway to the native structure. Moreover, we showed that under tension the intermediate exhibits unusual mechanical properties unfolding at low forces (only a few piconewtons) and displaying great compliance, deforming by 5 nm before unfolding, a property typical of structures stabilized by weak, non stereospecific tertiary contacts [31].

The data presented in Cecconi *et al.* and discussed in this paper demonstrate the power of direct mechanical manipulation to access processes that are difficult or impossible to examine with more traditional experimental approaches. By slowing down the folding/unfolding process of RNase H with force we were able to monitor and characterize an intermediate whose signal was concealed by time- and ensemble-averaging, and so could not to be directly observed in bulk experiments. Most significantly, we were able to characterize the mechanical properties of a molten globule structure. The experimental method presented here represents a completely new approach to single molecule manipulation studies and sets the stage for many new future experiments.

REFERENCES

[1] COHEN F. E. and KELLY J. W., *Nature*, **426** (2003) 905.
[2] DOBSON C. M., *Nature*, **426** (2003) 884.

[3] Baldwin R. L., *J. Biomolec. NMR*, **5** (1995) 103.
[4] Fersht A. R., *Structure and Mechanism in Protein Science: a Guide to Enzyme Catalysis and Protein Folding* (W.H. Freeman, New York) 1999.
[5] Strick T. *et al.*, *Phys. Today* **54**, issue no. 10 (2001) 46.
[6] Rief M. *et al.*, *Science*, **276** (1997) 1109.
[7] Rounsevell R., Forman J. R. and Clarke J., *Methods*, **34** (2004) 100.
[8] Yang G. L. *et al.*, *Proc. Natl. Acad. Sci. U.S.A.*, **97** (2000) 139.
[9] Brockwell D. J. *et al.*, *Nat. Struct. Biol.*, **10** (2003) 731.
[10] Carrion-Vazquez M. *et al.*, *Nat. Struct. Biol.*, **10** (2003) 738.
[11] Carrion-Vazquez M. *et al.*, *Proc. Natl. Acad. Sci. U.S.A.*, **96** (1999) 3694.
[12] Fernandez J. M. and Li H. B., *Science*, **303** (2004) 1674.
[13] Lee G. *et al.*, *Nature*, **440** (2006) 246.
[14] Cecconi C. *et al.*, *Science*, **309** (2005) 2057.
[15] Smith S. B., Cui Y. J. and Bustamante C., Optical-trap force transducer that operates by direct measurement of light momentum, *Methods in Enzymology*, vol. **361** (2003) pp. 134-162.
[16] Ashkin A. *et al.*, *Opt. Lett.*, **11** (1986) 288.
[17] Grier D. G., *Nature*, **424** (2003) 810.
[18] Svoboda K. and Block S. M., *Annu. Rev. Biophys. Biomol. Struct.*, **23** (1994) 247.
[19] Gordon J. P., *Phys. Rev. A*, **8** (1973) 14.
[20] Smith S. B., *Stretch Transitions Observed in Single Biopolymer Molecules (DNA and Protein) using Laser Tweezers*, Doctoral Thesis, University of Twente, The Netherlands, (1998).
[21] Cecconi C. *et al.*, Protein-DNA chimeras for single molecule mechanical folding studies with the optical tweezers, in preparation.
[22] Grassetti D. R. and Murray J. F. Jr., *Arch. Biochem. Biophys.*, **119** (1967) 41.
[23] Pedersen A. O. and Jacobsen J., *Eur. J. Biochem.*, **106** (1980) 291.
[24] Riener C. K., Kada G. and Gruber H. J., *Anal. Bioanal. Chem.*, **373** (2002) 266.
[25] Black C. B. and Cowan J. A., *Inorg. Chem.*, **33** (1994) 5805.
[26] Yang W. *et al.*, *Science*, **249** (1990) 1398.
[27] Dabora J. M. and Marqusee S., *Protein Sci.*, **3** (1994) 1401.
[28] Raschke T. M., Kho J. and Marqusee S., *Nature Struct. Biol.*, **6** (1999) 825.
[29] Raschke T. M. and Marqusee S., *Nature Struct. Biol.*, **4** (1997) 298.
[30] Parker M. J. and Marqusee S., *J. Mol. Biol.*, **293** (1999) 1195.
[31] Liphardt J. *et al.*, *Science*, **292** (2001) 733.
[32] Bustamante C. *et al.*, *Science*, **265** (1994) 1599.
[33] Spudich G. M., Miller E. J. and Marqusee S., *J. Mol. Biol.*, **335** (2004) 609.
[34] Kellermayer M. S. Z. *et al.*, *Science*, **276** (1997) 1112.